5
Transmission of Polarization Encoded Qubits in Optical Fibers

5.1.
Introduction

The first experimental demonstration of QKD was done over a 30-cm free-space distance using polarization encoding [76]. There were some experiments with polarization encoding in optical fibers [65], however due to residual birefringence in optical fibers, phase encoding was adopted [66, 67]. Phase encoding became the dominant for of transmission in optical fibers [68, 69]. Free-space QKD has still used polarization encoding extensively however [59, 118].

Interestingly polarization encoding usage in optical fibers has grown in recent years [98, 125, 126, 127, 128, 129, 130, 131], and this trend is expected to grow. Some of them employed active polarization control [98, 128, 131], however all of these control methods are time-multiplexed with the key transmission. Another interesting way to make the transmission polarization insensitive is to make use of the idea of decoherence-free subspaces [22]. When any linear combination of the entangled states $\left|\psi^{+}\right\rangle$ and $\left|\psi^{-}\right\rangle$ are transmitted in an optical fiber, they are immune to birefringence fluctuations (as long as both photons are measured), and thus well suited for polarization encoded QKD [132]. However, the requirement to generate and detect both photons increase the complexity of the source and of the detection system, as well as being more sensitive to fiber loss [129].

An active polarization control system was developed within our group recently [78]. It differs from the control schemes used above in the sense that it operates continuously because it is wavelength multiplexed. It has the advantage of being able to compensate very fast birefringence fluctuations in the fiber, such as those present in aerial cables. The experiment was performed together with the group of Nicolas Gisin from the University of Geneva as a joint collaboration [133].

PUC-Rio - Certificação Digital Nº 0510513/CA

5.2. Control theory

Work on the idea of active polarization control for QKD began as early as 2005, from some simulation results showing that very closed spaced wavelengths have a high correlation in respect to rotations induced from birefringence fluctuations [134]. Since a control system obviously requires a feedback, why not use a classical channel close to the wavelength of the quantum bits to supply the necessary information? Early tries were made using a single control channel as feedback, however results were unsuccessful because we came to the conclusion that one single channel (containing a single element of information, which is simply the intensity of the light after a polarizer) was only enough to control orthogonal states. The conclusion was made that two channels were needed (each channel launched in the fiber with non-orthogonal polarizations) for full real-time control. Indeed we built such a system later using this idea [78].

BB84 using polarization encoding requires that four states are sent, typically $|H\rangle$, $|V\rangle$, $|+45\rangle$ and $|-45\rangle$. In an optical fiber the relation between the output polarization state and the input one is given by where U_F is the unitary operator representing the rotations caused by random birefringence fluctuations in the fiber. As shown in [78] feedback provided by two reference channels is enough to perform the unitary transformation U_T, where $U_T = U_F^{-1}$. This transformation undoes the unitary rotation caused by the fiber such that the output quantum state is: $|\psi\rangle_{OUT} = U_T U_F |\psi\rangle_{IN} = |\psi\rangle_{IN}$.

As we have mentioned, the two classical control channels have a different wavelength than the quantum channel, and in fact U_F is wavelength dependent. Therefore we can intuitively think that the control cannot be perfect since the unitary transformations for control and quantum wavelengths will be different. While it may not be perfect, under certain conditions *good enough*. As we have shown, as long as the fiber mean group delay is of the order of 1 ps or less, and the channel spacing is sufficiently small (0.8 nm), the QBER contribution due to the control system stays under 1 % during the vast majority of the time [78]. As was shown there are other possible control schemes [134], like using a single wavelength channel with two polarization components split within two amplitude

PUC-Rio - Certificação Digital Nº 0510513/CA

modulation frequencies, or combining both the wavelength separation method with the double amplitude modulation frequency within a single channel method, and taking the mean result. This method yields the best possible results, however it requires a more complex setup. We opted to use the wavelength separation option using two channels with no amplitude modulation as it is conceptually simpler to implement. It naturally fits in the ITU-T wavelength grid with channel spacing of 0.8 nm (Fig. 37). It also gives the same control performance as the method with a single channel and the double amplitude modulation according to simulations performed [135].

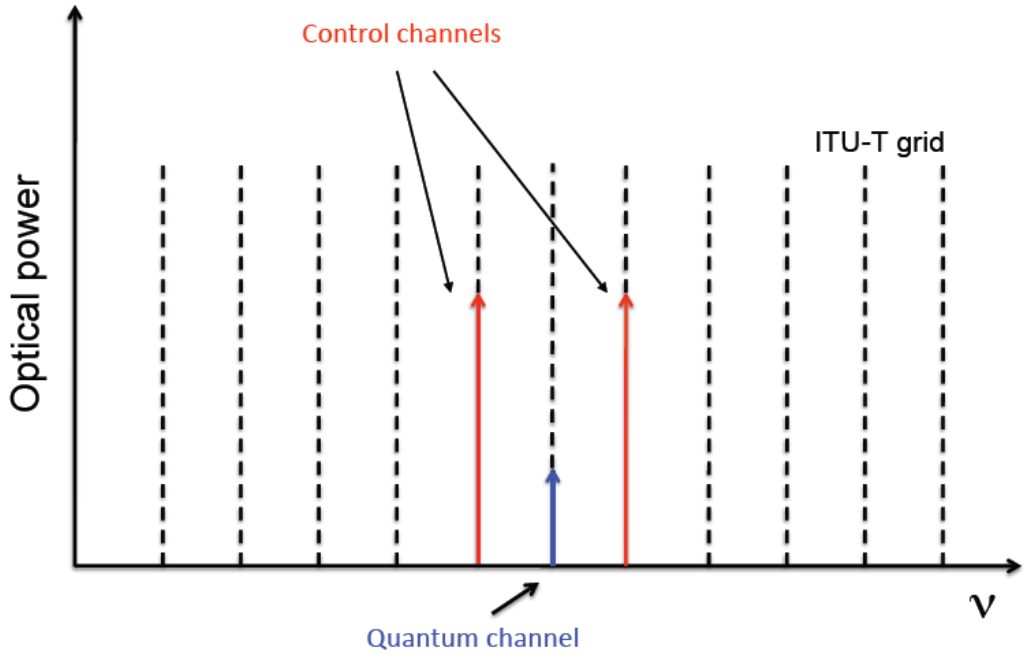

Figure 37 - Schematics showing the I_TU-T frequency grid (dashed black lines), the control channels (red) and the quantum channel (blue).

5.3. The experiment

The experiment is extensively based on the control system used in [78]. Based on the results of the Raman noise measurements presented in the previous chapter, one major change was needed. The original experiment was performed in a counter-propagating direction (single photons and classical channels work counter-propagatively). In that experiment noise was not a major issue because only a demonstration of the control scheme in the single-photon counting regime was required. For QKD, from our Raman measurements, the option to shut down

PUC-Rio - Certificação Digital Nº 0510513/CA

the side channel control lasers would not work counter-propagatively. Therefore we switched to a co-propagating configuration, even though the filtering requirements are steeper. The polarization control prototype was designed and assembled at PUC-Rio, fit in a standard 19-inch rack with 2U (units) height. It includes the optical components necessary for the polarization control, and the processing and driving electronics. The complete setup is shown in Fig. 38. The automatic polarization control system (APCS) is represented by the dashed orange line in the setup figure (A picture of the prototype is shown in Fig. 39). The electronics controlling the QKD setup supplied by the Geneva group is based on a previously used "plug and play" setup [68]. In the "plug and play" scheme Bob sends classical pulses to Alice, who then attenuates the signal to the single photon level, modulates them (including basis choice) and sends these attenuated pulses back to Bob, who finally performs his measurement basis choices and records the results from his detectors. Due to the "plug and play" configuration , Bob sends the trigger pulses to Alice, and the QKD electronics used in our experiment have to work in this way. Therefore we used a standard telecom DFB laser (Distributed Feedback) as the synchronization channel sending pulses from Bob to Alice (λ_S = 1547.72 nm) counter-propagating with the quantum and classical control channels.

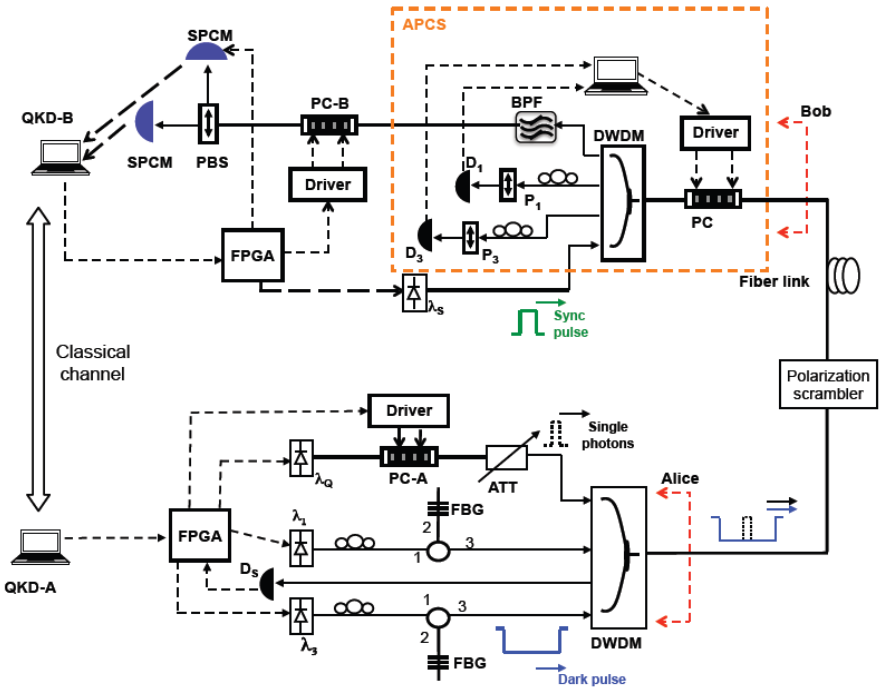

Figure 38 - Experimental setup for the polarization encoded QKD experiment. QKD-A and QKD-B: Alice and Bob's computers; FPGA: Field programmable gate array; D_S, D_1 and

PUC-Rio - Certificação Digital Nº 0510513/CA

D_3: Classical detectors; FBG: Fiber Bragg grating; PC-A and PC-B: Alice and Bob's $LiNbO_3$ polarization controllers; ATT: Optical attenuator; DWDM: Dense wavelength division multiplexer; P_1 and P_3: Polarizers; BPF: Band-pass filter; PBS: Polarizing beam splitter; SPCM: Single photon counting module. APCS: Automatic polarization control system. Solid lines represent optical fibers, while dashed ones are electrical connections. The direction of pulses is indicated in the figure.

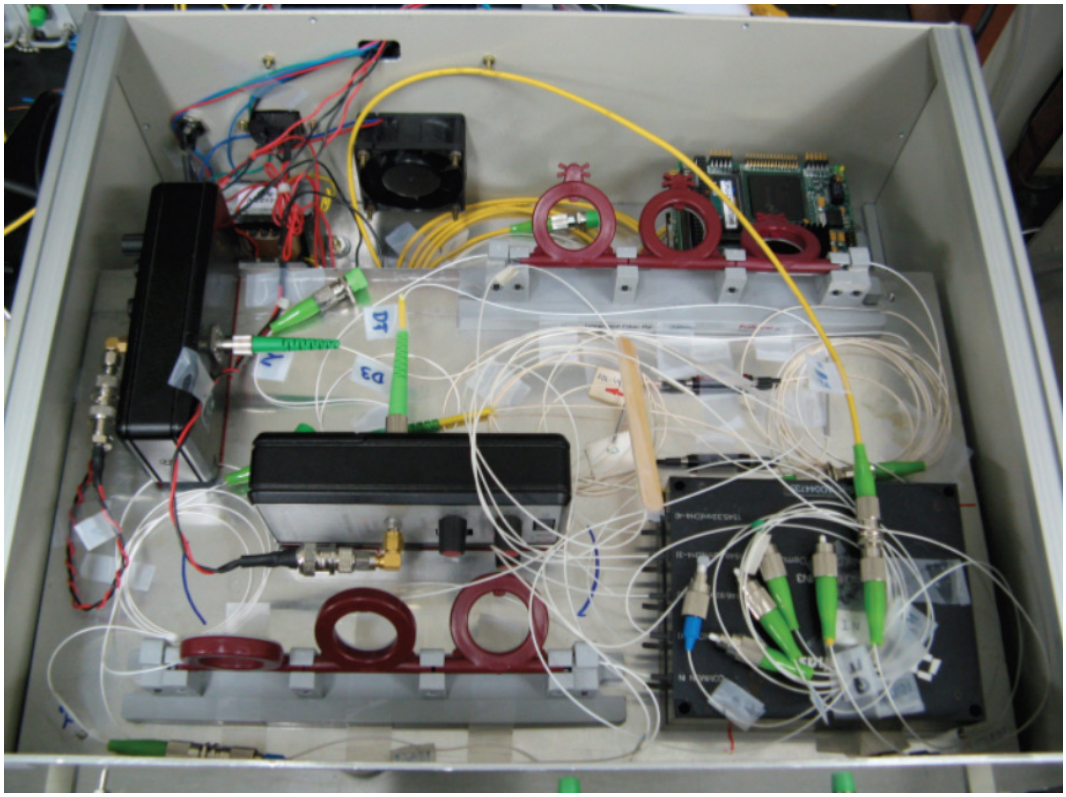

Figure 39 - Picture of the prototype. Clearly visible are the optical components: The polarization controllers, polarizers, detectors and the DWDMs. The electronics (power supplies, drivers and control CPU) are underneath the optics and thus not shown.

The two classical control channels are also composed of DFB lasers at wavelengths λ_1 = 1545.32 nm and λ_3 = 1546.92 nm. The quantum channel uses a pulsed attenuated DFB laser centered at λ_Q = 1546.12 nm. All three channels are multiplexed at Alice's setup using a commercial DWDM multiplexer with 1.4 dB insertion loss and an extinction ratio of at least -35 dB between adjacent channels and -45 dB between non-adjacent ones. Each side channel employs a circulator with a FBG centred at λ_Q to remove any ASE noise generated from the respective lasers, which would fall on the SPCM at Bob's side, rendering QKD impractical. A measurement of the spectra of the DWDMs is shown in Fig. 40.

PUC-Rio - Certificação Digital Nº 0510513/CA

As discussed before there are two main noise contributions we need to counter in order to perform a successful QKD session. The first is caused by "real" components, such as filters with finite extinction ratios and lasers emitting light outside of their center wavelength. The second contribution comes from the fiber itself, in the form of non-linear effects (Alice and Bob are connected by 16 km of standard optical fibers in our experiment) . The circulators with the Bragg gratings and the DWDMs used in the setup took care of the noise coming from cross-talk and imperfect components. In order to remove the Raman spontaneous contribution (the main form of in-fiber generated noise in our case), we created a short dark slot, in which the pseudo-single photon pulse is transmitted, of 13.5 ns by suppressing the laser current thus reducing the power to -90 dBm. We took this approach since, as mentioned in Chapter IV, the Raman spontaneous scattering induced is linear, and thus harder to remove by simply attenuating. Our method completely removes the Raman noise contribution, and it does not compromise the control performance since we use a low-pass filter on the detection side (not shown in Fig. 38). Fortunately for this experiment, the Raman noise contribution according to our measurements is smallest the closer the spacing between the classical and quantum channels (Fig. 41).

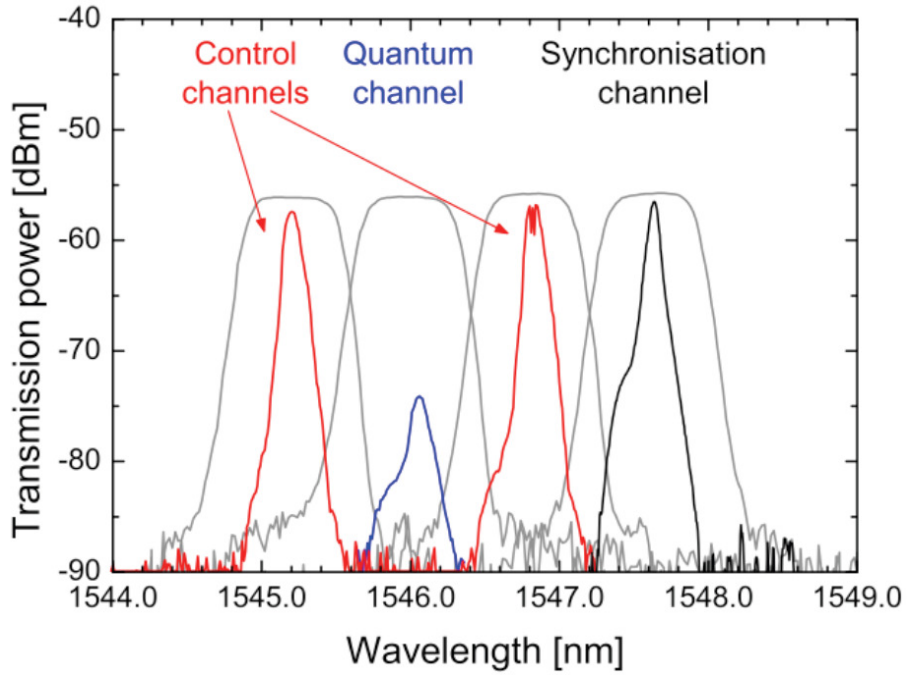

Figure 40 - Emission spectra of the two polarization control lasers (red), quantum channel laser (blue) and synchronization laser (black) aligned to 4 adjacent channels of the ITU-T band between 1545.32 and 1547.72 nm. The transmission spectra of the respective DWDM channels are shown as grey lines. Measurement performed by N. Walenta.

PUC-Rio - Certificação Digital Nº 0510513/CA

To temporally synchronize with Alice, Bob generates 1 ns long pulses with a repetition frequency of 5 MHz. These clock signals are transmitted in trains of 300 pulses in the same fiber as the quantum and classical side channels to Alice using a DFB laser centered at λ_Q = 1546.92 nm. In principle, backscattered photons from the synchronization pulses would induce noise in the quantum channel due to Raman and crosstalk from Rayleigh backscattering. However, these effects are not relevant in our setup since, at Alice, we delay the incoming signals by 50 ns in order to gain time to synchronize her internal clock with the incoming pulses before triggering the emission of the quantum signals. This delay acts as storage for the synchronization pulses such that no intersection of quantum signals and backscattered light takes place in the transmission fiber. We verified that the synchronization pulses did not affect the noise on the SPCMs at Bob.

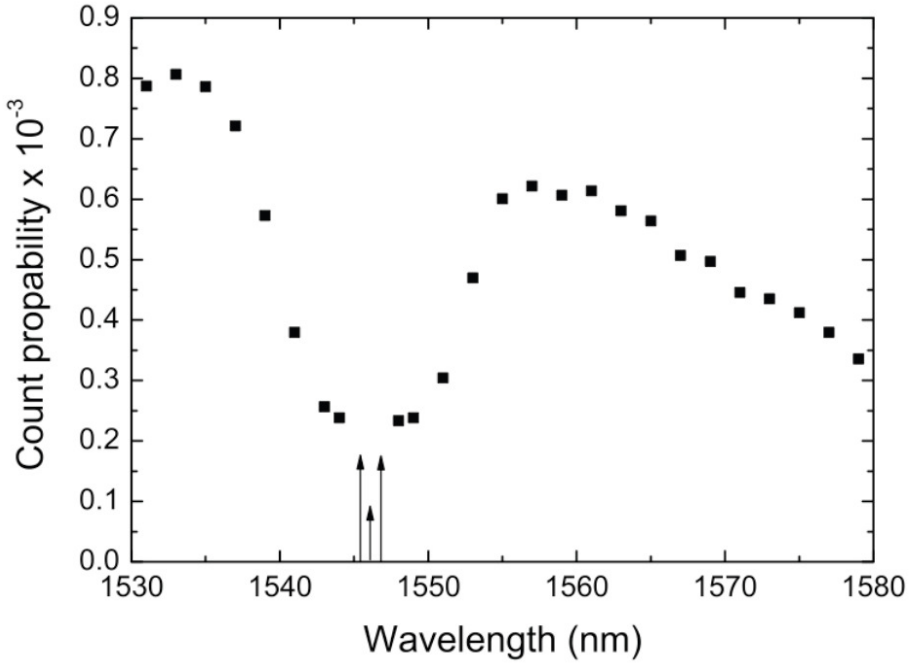

Figure 41 - Zoomed version of Fig. 27. The three arrows at the bottom represent the classical and quantum channels.

The SOP (State of polarization) of the faint laser pulses is modified with a fast $LiNbO_3$ fiber pig-tailed electro-optic polarization controller (PC-A, EOSPACE), with the modulating electrical signal generated from a FPGA (Field Programmable Gate Array) passing through a high voltage electronic driver (V_π approximately 50 V). This controller switches between the four distinct SOP needed in the BB84 protocol. An identical set of $LiNbO_3$ controller and driver is

PUC-Rio - Certificação Digital Nº 0510513/CA

used by Bob to change between the two measurement bases (PC-B). The modulator in our setup was able to change between orthogonal polarization states within 10 ns, as shown in Fig. 42. This measurement was performed by modulating the polarization state of a CW laser with one of the $LiNbO_3$ controllers, passing the optical signal through a polarizer and measuring the signal intensity with a p-i-n photodiode. From this we verify that our modulation speed is compatible with the 5 MHz repetition frequency generated from the electronics.

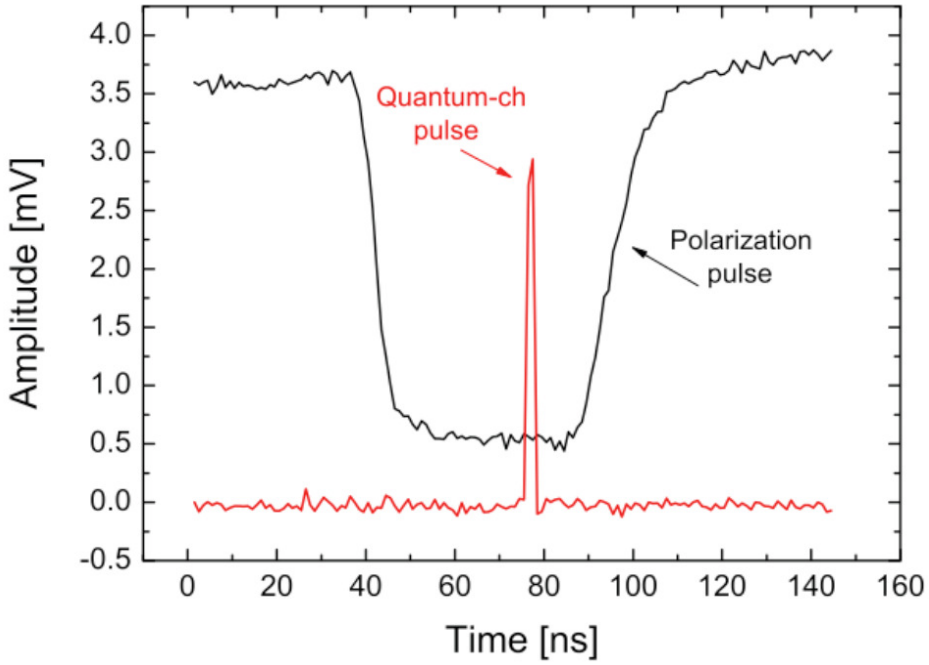

Figure 42 - Intensity measurements of a polarization pulse (black), and the quantum channel signal (red), operating on classical power levels. The polarization pulse was taken after a polarizer, with a CW laser, while switching the SOP between two orthogonal values, and back to the original. The quantum channel pulse is included here as a reference, showing that it is much narrower than the polarization bit. Measurement performed by N. Walenta.

The classical side channels are separated by the DWDM and pass through linear polarizers with their optical axis adjusted to be non-orthogonal using manual polarization controllers [78]. Their optical intensities after the polarizers are measured by classical p-i-n photodiodes and fed to the control computer for processing. Its control algorithm maximizes the intensity of both control channels at the same time by changing the polarization state of the optical signals before splitting at the DWDM. By maximizing both side channel intensities simultaneously the original input polarization states are recovered. The whole

PUC-Rio - Certificação Digital Nº 0510513/CA

setup is controlled by personal computers that send out the necessary electrical signals to the optical components to perform a QKD session, and perform the classical procedures required by BB84. The classical channel between Alice and Bob was realized with an USB connection between both systems.

Before performing a quantum transmission, the entire setup is calibrated by adjusting the polarization of the quantum channel as well as both side channels. For the quantum channel, two manual polarization controllers (not shown in Fig. 38) before PC-A and PC-B were used to align the input polarization state with the $LiNbO_3$ polarization modulator for identical maximum rotations on the Poincaré sphere. Another manual polarization controller (also not shown in figure 38) is placed at Bob after his PC-B to align the state to the axis of the subsequent polarizer.

The polarization states of the side channel lasers were set with two manual controllers to be non-orthogonal. We have improved on the previous scheme in such a way that the control will work properly as long as the side-channels are non-orthogonal, but not necessarily maximally overlapped as it used to be the case [78], which makes the system more robust and considerably easier to align than before. The alignment procedure only needs to be done once, before initializing the transmission. We note that this adjustment could be performed automatically by employing additional $LiNbO_3$ controllers, and as such, our system could be used in a commercial environment where no manual intervention is needed.

After alignment of the entire system we tested the performance of the setup initially with the stabilization system installed but not active. Alice's quantum signals were attenuated to obtain an average of μ = 0.1 photons per pulse. With a side channel laser power of -7.4 dBm each, but without the stabilization system running and the polarization scrambler turned off, the prepared states yielded a visibility of 97.2 % corresponding to a minimal QBER of 1.4 %. The measured QBER was 1.6 %, with an optical share $QBER_{opt}$ = 0.7 % which is caused by the detection of photons in the wrong detector, mainly due to the limited 22 dB extinction of Bob's polarizing beam splitter. Another share of $QBER_{det}$ = 0.1 % is caused by noise counts due to the SPCMs and a share of $QBER_{side}$= 0.8 % is caused by noise due to crosstalk and photons generated by Raman scattering in the side channels. With the stabilization system active, the total QBER increased by 1.1 %. This can be ascribed to an increase in the optical

PUC-Rio - Certificação Digital Nº 0510513/CA

share $QBER_{opt}$ due to fluctuations of the polarization state inherently induced by the stabilization algorithm.

Before demonstrating QKD we characterize the performance of the stabilization system even in the presence of fast polarization changes using the scrambler. A voltage ramp can be applied to each piezo crystal, which performs a polarization rotation of 2π back and forth on the Poincaré sphere at a tunable frequency. As such, a scrambling frequency of 1 Hz means a polarization rotation of 4π per second. It should be noted that such extreme polarization fluctuations are rarely expected in normal environments.

In order to reduce the influence of detector and side channel noise to less than 0.1 % during the following characterization, we increase the average photon number to μ = 1.0 per pulse. We constantly prepare the same state at Alice and measure in the corresponding basis at Bob, in order to eliminate any possibility of errors induced by the polarization modulators. Figure 43 then shows the optical share $QBER_{opt}$ measured at different voltage ramp frequencies applied to the scrambler. Each point is averaged over 50 measurements, with 1 million photon pulses sent from Alice to Bob per measurement. The results show that $QBER_{opt}$ stays constantly under 6 % for scrambling frequencies up to 16 π/s, and increasing the rotations to 40 π/s, $QBER_{opt}$ has an average of 7.5 %, well below the limit of 11% [7].

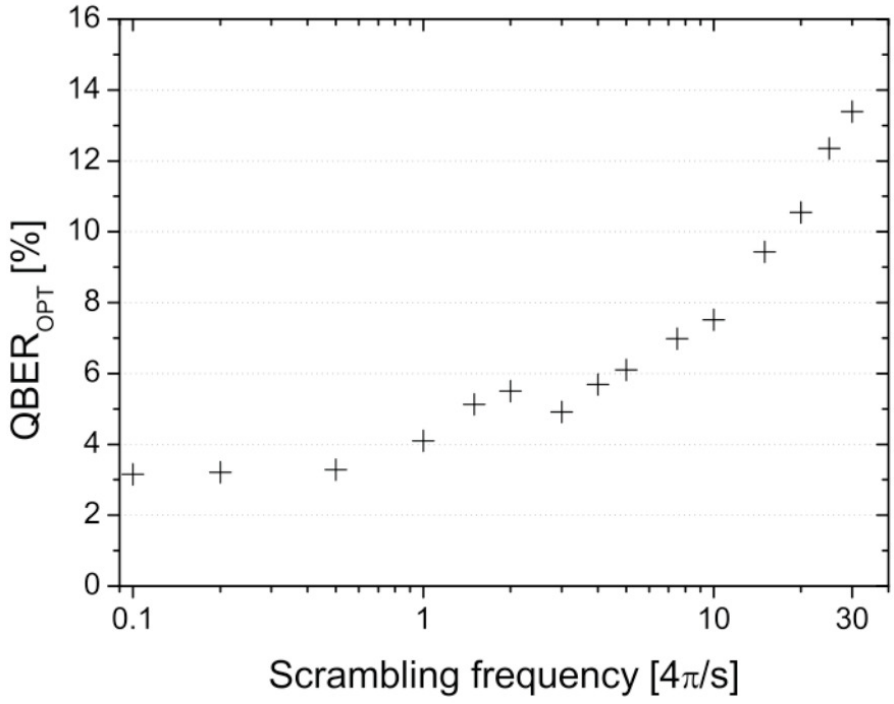

PUC-Rio - Certificação Digital Nº 0510513/CA

Figure 43 - The optical share $QBER_{opt}$ as a function of the scrambling frequency demonstrating the stabilization capability of the control system under rapid polarization changes. Each value is averaged over 50 measurements, with 1 million photon pulses sent per measurement. Measurement performed by N. Walenta.

To demonstrate the applicability of the stabilization system for QKD under the condition of random polarization changes, as it occurs in aerial fibres or under thermal or mechanical stresses, we replaced the piezo-electric scrambler by a manual polarization modulator. Unfortunately, an electronic problem with Bob's polarization modulator PC-B reduced the stability and extinction of its modulation during a key exchange at 5 MHz. This forced us to simulate a random key exchange by measuring Alice's randomly prepared qubits first in one basis at Bob and then, in a subsequent measurement, in the other basis. In Fig. 44 both measurements are combined on top of each other with black points indicating key exchanges with measurements in Bob's first basis and red points in the second, respectively. This problem, along with errors in the alignment, is also the reason for the slightly increased QBER during the key exchange demonstration.

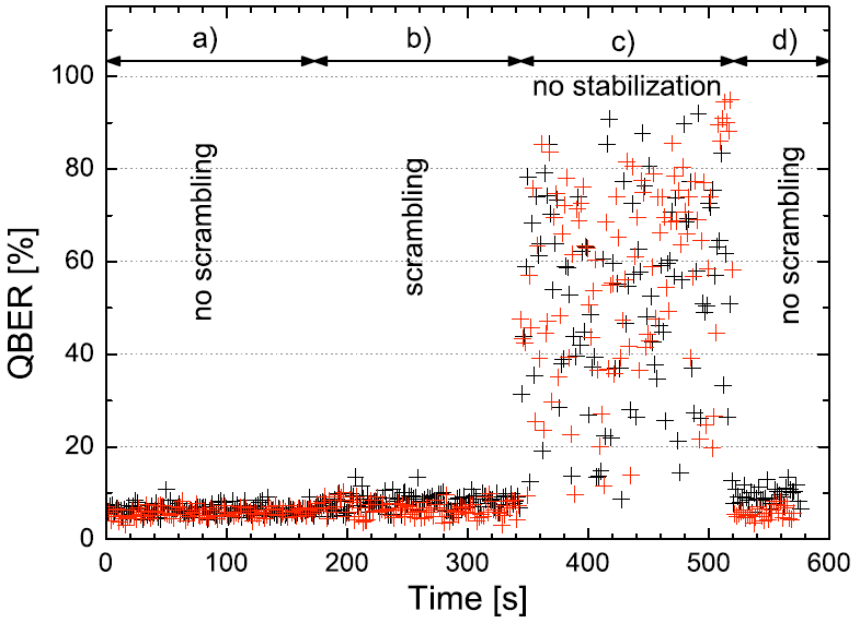

Figure 44 - QBER as a function of time under different conditions. a) No polarization scrambling. b) Polarization scrambling with active stabilization. c) Polarization scrambling without stabilization system. d) Re-stabilization after the system is reactivated. Each point corresponds to 1 million sent qubits. Black and red points distinguish measurements in different bases at Bob (see text for details). Measurement performed by N. Walenta.

PUC-Rio - Certificação Digital Nº 0510513/CA

Still, figure 44 shows the effectiveness of the stabilization system when the polarization state is randomly scrambled in the order of a few rad/s. Again, each point represents a key exchange of one million sent qubits. In the first section of the figure, (part a) keys are distributed with the stabilization system running but without any polarization scrambling. In the second section (part b) the average QBER increases by only 1.2 % during the key exchange although the polarization states are continuously and randomly scrambled. By comparison, without the stabilization system the QBER would increase dramatically with an average of around 50 % (part c) making any quantum key distribution impossible. The last section (part d) reveals that the system is able to re-stabilize immediately when it is reactivated.

The scheme implemented here demonstrates that it is possible to achieve real-time continuous control of the polarization state of single photons along a 16 km long optical fiber link, with an active polarization scrambler connected in series. We have demonstrated the feasibility of quantum key distribution employing polarization encoded qubits in optical fibers, in situations where the SOP of the transmitted photons is subject to fast random variations. The scheme was assembled using only standard off-the-shelf telecom components, and can be used with other single-photon sources, such as those based on SPDC. Furthermore our setup allows other applications requiring polarization encoding in long-distance quantum communications in optical fibers.

PUC-Rio - Certificação Digital Nº 0510513/CA